Temperature Effect on Viscoelastic Properties of Anisotropic Magnetorheological Elastomer in Compression

Yanxiang Wan[1,a], Yeping Xiong[1,b], Shengming Zhang[2,c]

[1]University of Southampton, UK
[2]Lloyd's Register, UK
[a]yw8g12@soton.ac.uk, [b]Y.Xiong@soton.ac.uk, [c]Shengming.Zhang@lr.org

*Yanxiang Wan

Key words: Magnetorheological elastomers, dynamic mechanical analysis, viscoelastic properties, temperature effect, time-temperature superposition.

Abstract: Magnetorheological elastomers (MREs) are a class of smart materials composed of an elastomer and micron-sized magnetic particles. Besides the loading amplitude and frequency, the elastic and rheological properties of MREs are also dependent on the external magnetic field and temperature. Previous studies focused on the influences of external magnetic field, strain amplitude and frequency on the dynamic properties, however, the temperature effect was rarely reported. In this paper, the dynamic mechanical analysis (DMA) tests were carried out to investigate the viscoelastic properties of the anisotropic MRE samples under various temperatures and magnetic fields. A transition behavior of the anisotropic MRE samples was observed at about 50°C for dynamic modulus. The storage modulus initially decreased with the increasing of temperature up to 50°C and then increased or maintained a stable value when temperature increased until to 60°C. The time-temperature superposition (TTS) principle was extended to construct the dynamic modulus master curve of the MREs by using the horizontal shift factor and the vertical shift factor. The good correlations between the measured and predicted data were confirmed by performing statistical analysis for the goodness of fit. The constructed master curve and shift factors can be used to predict the viscoelastic properties of the MREs beyond the DMA experiment range of temperatures and frequencies.

1 Introduction

Magnetorheological elastomers (MREs) show the potential application in semi-active vibration control due to their dynamic properties that can be adjusted rapidly and reversibly by changing the external magnetic field [1-4]. It is well known that the dynamic mechanical properties of MREs are affected not only by its components and the fabrication process [5-7] but also by the in-service conditions such as load amplitude, excitation frequency, external magnetic field, and temperature etc. [8-11]. In order to achieve an optimal damping or vibration isolation system for practical application of MRE based active or semi-active vibration control device, the characterization and modelling of MREs under various load conditions are essential to be determined.

There have been several existing models so far for describing the dynamic properties of MREs under the combination of magnetic and mechanical load conditions. Among these modeling approaches, the parametric model has received considerable attention due to its efficient and rapid simulation of the dynamic behaviors of MRE based devices under various loading conditions. The magnetic field induced stiffness of MREs was described by using a nonlinear spring element connected in parallel with a linear viscoelastic model [12-14]. In order to take account for the effects of the interfacial friction in high frequency range, a spring-Coulomb friction slider and smooth frictional elements were used in a nonlinear constitutive model [15, 16]. The nonlinear hysteresis behavior of MREs in large amplitude excitation was modeled by the Ramberg-Osgood model, the Bouc-Wen model, and the Prager model respectively in parallel with the classic viscoelastic model [17-19].

Recently, a new viscoelastic model was developed by dividing the dynamic shear modulus of MREs into mechanical and magnetic parts [20]. The mechanical shear modulus was calculated by the

Kraus model and the influence of magnetic field on the shear modulus was described by the relative magnetorheological (MR) effect, which was affected by the strain amplitude and magnetic flux intensity. A modified Kelvin-Voigt model was presented to describe the nonlinear relationships between the shear stress and shear strain of MREs under external magnetic field [21]. In this model, the stiffness of spring and the damping of dashpot were dependent on the magnetic flux, strain amplitude and frequency. The storage and loss moduli were modeled by using power function of strain amplitude and frequency. The magnetic field dependent parameters in the proposed model were expressed by polynomial functions with five parameters of which two are independent of magnetic field. The other three can be expressed by the quadratic and linear using nonlinear regression.

A mechanical model was proposed for modeling of a multilayered MRE isolator based on the combination of the dynamic equations, constitutive models, and electromagnetic analysis [22]. In each layer, the relationship between shear stress and shear strain was modeled by the Kelvin-Voigt model and the Bouc-Wen model in parallel. The model parameters of the constitutive models were identified by electromagnetic analysis results. The fractional Zener model was used to describe the frequency dependent dynamic properties of anisotropic MREs under external magnetic field [23]. In this model, the magnetic field induced dynamic shear modulus was predicted base on the dipole model. The capability of various fractional viscoelastic models was examined for the magnetoactive elastomer in a wide range of magnetic fields [24]. The results showed that the viscoelastic models with one fractional element can adequately describe the rheological behavior of the magnetoactive elastomer under low and for some cases high magnetic fields. The viscoelastic models with more fractional elements were needed to describe the rheological properties of the magnetoactive elastomer under intermediate magnetic fields.

The elastic and rheological properties of MREs in addition to an applied magnetic field are also dependent on the thermal-mechanical load conditions. The temperature has an important effect on material properties of MREs and the performance of MRE based devices [10, 11], as well as composite materials and structures [25, 26]. Compared with the extensive research on the parametric modeling of the frequency-, amplitude-, and magnetic field-dependent viscoelastic properties of MREs, to our knowledge, there is a limited number of published studies on the parametric modeling of the temperature-dependent viscoelastic properties of MREs. This may be due to the fact that MREs are multi-phase composites and usually behave the characteristics of the thermorheologically complex materials.

The relationship between frequency and temperature, named master curve, can be established by the time-temperature superposition (TTS) principle for the thermorheologically simple materials such as single-phase, single-transition amorphous homopolymers and random copolymers [27]. The elastic constants are independent of temperature and the time constants have the same dependence of temperature. The isotherms of dynamic modulus can be shifted into a smooth master curve by using the horizontal shift factor. The master curve constructed by TTS principle has been successfully applied to predict the elastic and rheological properties of viscoelastic materials over a range of frequencies within linear viscoelastic region [28-30]. At the same time, many research efforts were delivered to extend the application of TTS to multi-phase composites that the deviations from the thermorheologically simple behavior are not too large [31-33]. The results revealed that the TTS principle does not hold for a multi-phase system in general but does hold for a multi-component system in which all components have the same temperature dependence and identical shift factors, or some components have the same temperature dependence and the others have no or nearly no temperature dependence [32, 33]. An unexpected result was that the storage modulus of iron particle filled poly (norbornene) (PNB) was independent on the iron particle content and the PNB represented a perfectly thermorheologically simple material behavior. The master curve presented a good fit for the storage modulus and loss factor of the PNB with varying contents of spherical iron particles. A phenomenological frequency-temperature shift was presented with a good fit for storage modulus of poly (dimethylsiloxane) (PDMS) filled with varying contents of spherical iron particles. Although the PDMS was not thermorheologically simple material, but it was linearly dependence of temperature

and had the same shift factor [33]. The dynamic modulus master curve of an isotropic magnetosensitive elastomer in the absence of magnetic field and the magnitude of complex modulus master curve of an MR fluid under magnetic field were constructed respectively in the literature [34, 35] however the statistical analysis of the good-of-fitness were not presented. There is a research gap on the dynamic modulus master curve of anisotropic MREs in the presence of magnetic field.

In this paper, a series of DMA tests have been carried out to investigate the viscoelastic properties of anisotropic MREs under different temperature and magnetic fields. The logarithmic Cole-Cole plot and the semi-logarithmic Black diagram were depicted to verify whether the TTS principle can be used to construct the master curve of the MRE samples or not. The fractional Zener model was employed to describe the elastic and rheological properties of the MREs based on the obtained experimental data. The dynamic modulus master curve of the MRE sample was constructed by the horizontal and vertical shift factors based on TTS principle. Finally, the statistical analysis of goodness-of-fit is performed for various shift factors and viscoelastic models. The good correlations between the measured and predicted data have been evaluated by the statistical analysis results.

2 Experimental

According to the BS ISO 4664-1:2011, the dynamic mechanical analysis (DMA) tests have been carried out to investigate the dynamic properties of MRE samples under uniaxial harmonic compressive loading in the Transport Systems Research Laboratory. The anisotropic MRE samples used in this study were synthesized from silicone rubber (Elastosil A and Elastosil B, Wacker Chemie AG, Germany) and micron-sized iron particles (grain size 5-9 μm with ≥99.5%, Sigma-Aldrich, US). The anisotropic MRE samples with the particle volume fraction of 30% were prepared in room temperature and external magnetic field based on the published experiment results of MREs that the magnetorheological (MR) effect of anisotropic MREs is slightly larger than isotropic MREs [36, 37] and the maximum MR effect is normally achieved when the iron particle volume fraction is about 30% [38, 39].

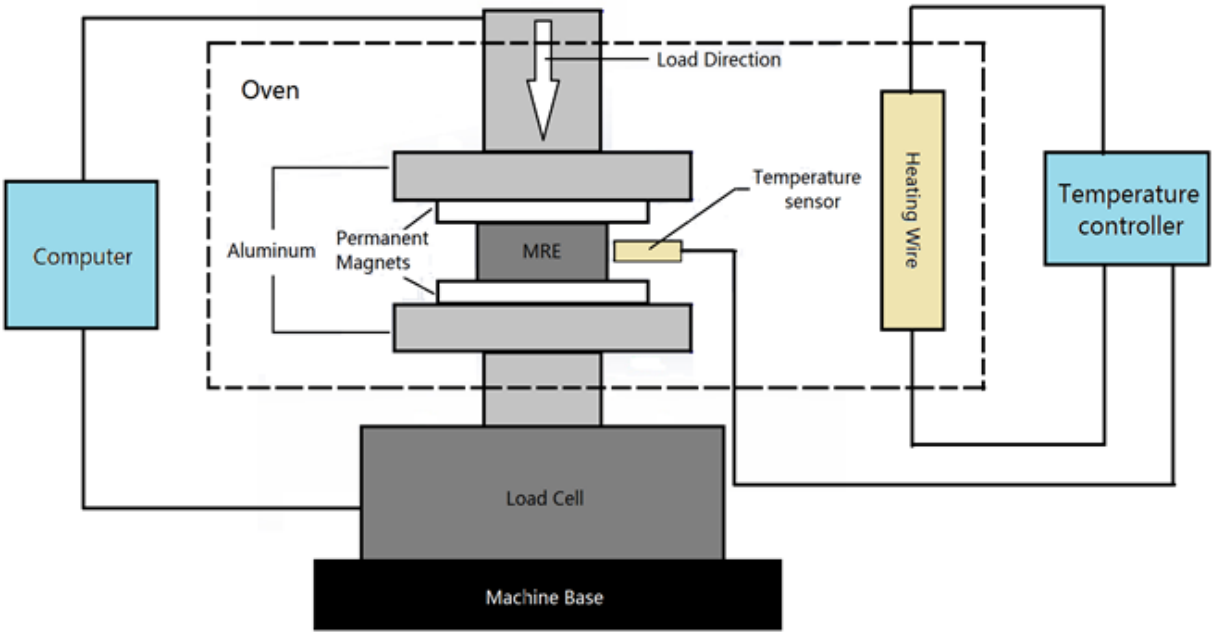

(a)

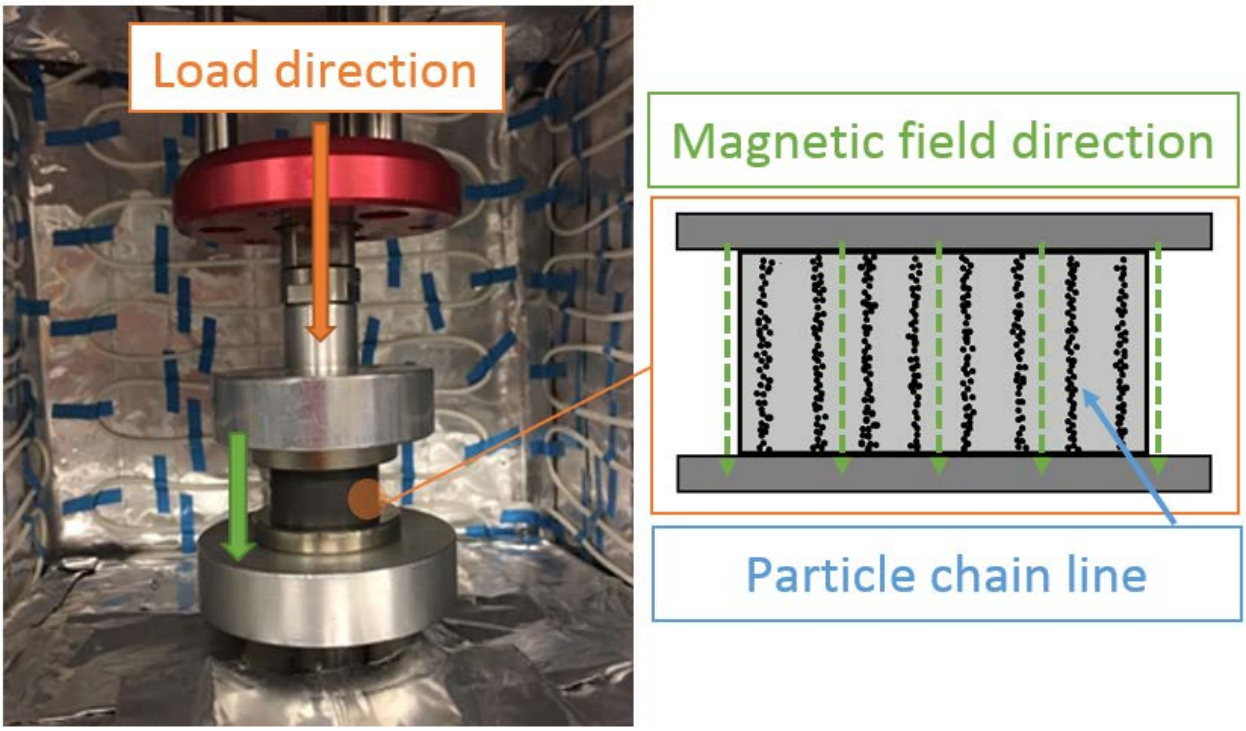

(b)

Figure 1. Experiment setup for DMA test of MRE sample under uniaxial compression.

The experimental setup consists of the Instron test machine (E1000 Electro plus), a self-manufactured oven and the pairs of the cylindrical grad N42 neodymium permanent magnets (E-magnets, UK) as shown in Figure 1. The magnetic field was generated by a pair of the cylindrical grade N42 neodymium permanent magnets. The environmental temperature inside oven was controlled by a self-manufactured oven comprised of the heat insulation layer, the heating wire, a thermo detector, and a temperature control panel. The Instron test machine (E1000 Electro plus) applied the uniaxial harmonic compressive loading to the MRE specimen. The strain amplitude and the excitation frequency were controlled through the displacement channel and the resulting force was measured by the force channel. The MRE samples were placed between two permanent magnets, the force direction is along with the magnetic field direction. This is also the same direction as the column chain line of the iron powder inside the MRE samples.

The DMA experiments were carried out to achieve the isothermal dynamic moduli of the MRE samples with different strain frequencies ranging from 1 to 60 Hz, temperatures varying from room temperature (about 25°C) to 60°C with the interval of 5°C, and different magnetic fields (0, 300 mT, and 500 mT). The strain amplitude was set to be less than or equal to 10% to obtain the linear viscoelastic response [12]. The larger MR effect can be achieved in the linear viscoelastic region [8].

Before the isothermal dynamic moduli were measured, the MRE samples were preloaded and unloaded for ten cycles to reduce the Mullins effect. Three pairs of the MRE samples were measured independently and DMA test was repeated twice for each pair of the MRE samples. The reliability of the experimental data was guaranteed by averaging the measurement data.

3 Modeling

3.1 Viscoelastic model

MREs belong to a class of smart composite materials composed of an elastomer and micron-sized magnetic particles. Their elastic and rheological properties in addition to the loading amplitude and frequency are dependent on the external magnetic field and temperature as shown in Figure 2 and Figure 3. The dynamic modulus of MREs can be modeled by linear viscoelastic models within small

strain range and in the presence of an applied magnetic field [12-14].

There are many viscoelastic models available in literature to describe the master curve of dynamic modulus. These models be categorized into two groups: the mechanical models and the mathematical models. The mechanical models (also called analogical models) simulate the elastic and rheological responses of viscoelastic materials by using a particular combination of springs and dashpots (or springpots) in series and/or parallel, e.g. the generalized Maxwell model, the generialized Kelvin-Voigt model and the fractional Zener model. While the mathematical models (also called empirical algebraic models) utilize an analytical expression to fit experimental data, such as the CAM model and the sigmoidal model.

In this paper, the fractional Zener model [40, 41] is adopted respectively to predict the dynamic modulus of MRE samples under the external magnetic field and unaxial harmonic compression. The complex modulus can be expressed as follows,

$$E^*(\omega,T) = E_0 + \frac{E_\infty - E_0}{1+(j\ \omega\tau)^\alpha} \tag{1}$$

in which, α is the order of the fractional derivative in the range of 0 to 1, τ is the generalized relaxation time dependence of the temperature, E_0 is the long time or relaxed modulus, and E_∞ is the unrelaxed or instantaneous modulus.

The coresponding storage modulus and loss modulus are,

$$E'(\omega,T) = E_0 + (E_\infty - E_0)\frac{(\omega\tau)^\alpha \cos\frac{\alpha\pi}{2} + (\omega\tau)^{2\alpha}}{1 + 2(\omega\tau)^\alpha \cos\frac{\alpha\pi}{2} + (\omega\tau)^{2\alpha}} \tag{2}$$

$$E''(\omega,T) = (E_\infty - E_0)\frac{(\omega\tau)^\alpha \sin\frac{\alpha\pi}{2}}{1 + 2(\omega\tau)^\alpha \cos\frac{\alpha\pi}{2} + (\omega\tau)^{2\alpha}} \tag{3}$$

The magnetic field induced dynamic modulus can be described by the relative MR effect on storage modulus and loss modulus respectively [13, 14, 20]. The existing experimental results revealed that the relative MR effect is mainly dominated by the dipole interaction force of magnetic particles in the presence of magnetic field [36-38]. Therefore the relative MR effect is mainly dependent on the magnetic flux density and can be expressed by quadratic function of magnetic flux density until the saturation of magnetization [16, 21].

3.2 Shift factor equations

The isothermal dynamic modulus, including storage modulus and loss modulus, can be shifted respectively into a unique master curve at a reference temperature when the applicable of the TTS principle has been verified [28-30].

$$E'(\omega_r, T_r) = b_T(T, T_r)\,E'(\omega,T) \tag{4}$$

$$E''(\omega_r, T_r) = b_T(T, T_r)\,E''(\omega,T) \tag{5}$$

$$\omega_r = a_T(T, T_r)\,\omega \tag{6}$$

Where, ω_r and T_r denote reduced frequency and reference temperature, $a_T(T,T_r)$ and $b_T(T,T_r)$ are the horizontal and vertical shift factors respectively.

The shift factor definition is mainly based on the observation that isothermal dynamic modulus curves obtained from DMA experiments can be shifted into a smooth master curve with the goodness of fit between measured and predicted data: higher value of the coefficient of determination (R^2) and lower value of the standard error ratio (S_e/S_y). The numerical shift factor for each isotherm of dynamic modulus produced the best fit between experimental and predicted data [42]. While the functional shift factor has an adventage over the numerical shift factor in mathematical expression and application to computer software [43]. In addition, if a functional form with some thermodynamic basis is used then the resulting master curve and shift factor equations can be employed to predict the viscoelastic behavior beyond the measurement data range of temperatures and frequencies. In general, the horizontal shift factor is commonly expressed by simple temperature dependent equations, such as the Arrhenius model and the WLF model of Williams-Landel-Ferry equation because of their strong thermodynamic basis, and the quadratic polynomial function for the sake of fitting accuracy [43, 44].

The Arrhenius equation and the WLF empirical equation:

$$\log a_T\left(T,T_r\right) = C\left(\frac{1}{T}-\frac{1}{T_r}\right) \tag{7}$$

$$\log a_T\left(T,T_r\right) = \frac{C_1\left(T-T_r\right)}{C_2+\left(T+T_r\right)} \tag{8}$$

in which, C , C_1, and C_2 are model parameters respectively, and T_r is the reference temperature chosen for the master curve.

and the quadratic polynomial function:

$$\log a_T\left(T,T_r\right) = a_1\left(T-T_r\right)+a_2\left(T-T_r\right)^2 \tag{9}$$

where a_1 and a_2 are model parameters.

The vertical shift factor represents temperature induced density changes and supplements for polymers with vertical shifts of the dynamic modulus [31, 45].

$$b_T\left(T,T_r\right) = \frac{\rho_r T_r}{\rho T} \tag{10}$$

in which, ρ and ρ_r are density of the material at current temperature, and reference temperature.

Where the temperature ratio represents an effect of entropy-based restoring force in the flexible chains and the ratio of density represents an effect of thermal expansion. The vertical shift factor is weakly dependent on temperature and is often neglected in most cases [45]. Under the assumptions about densities that the mass of the material remains constant when temperature varying, the approximations of vertical shift factor can be derived as follow [31].

$$b_T\left(T\right) \approx 1+b_1\left(T-T_r\right)+b_2\left(T-T_r\right)^2 \tag{11}$$

where b_1 and b_2 are model parameters dependent on reference temperature and the thermal expansion coefficient of the material.

4 Results and discussion

4.1 Experimental data and analysis

The isothermal dynamic properties of the MRE samples, including hysteresis loops and dynamic moduli, have been measured within small strain range in different temperatures and magnetic fields. According to the DMA experiments, it can be noticed that both the storage modulus and loss modulus

are almost linear decreased with the strain amplitude. This tendency does not change to o much with the environment temperature. For example, Figure 2 shows the magnetic field and temperature dependent hysteresis loops of the MRE samples under uniaxial harmonic compression with strain amplitude of 1% and frequency of 60 Hz. It can be observed from Figure 2 that each of the hysteresis loops formed an approximate elliptical shape, indicating the MRE sample behaves with linear viscoelastic properties [12]. The slope of the main axis of hysteresis loop was dependent on both magnetic field and temperature. However, it increased with the increasing of magnetic field but exhibited two different trends with the variation of temperature: it first decreased and then increased with the increasing of temperature. This is due to the transition behavior of the MRE stiffness occurred at about 50°C. The transition behavior of MREs is mainly related to the alpha phase transition of the silicon rubber matrix [10] and the variation of dipole interaction of magnetic particle due to temperature changes. According to differential scanning calorimetry (DSC) measurement result, the transition behavior began at about 50°C and reached the exothermic peaks at 58.66°C. This indicates that the MRE material started the phase transition at about 50 °C.

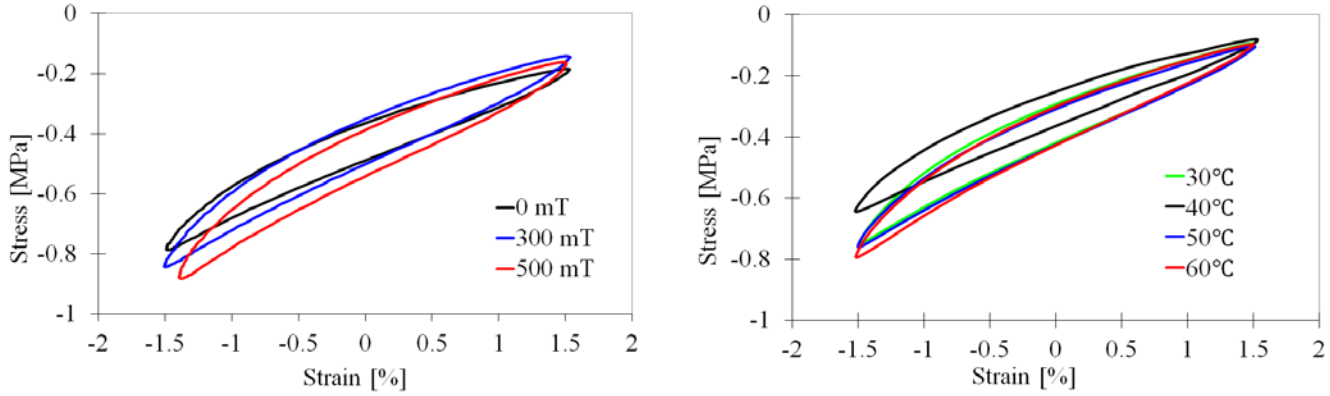

(a) (b)

Figure 2. Dependence of hysteresis loops on different: (a) magnetic fields, and (b) temperatures.

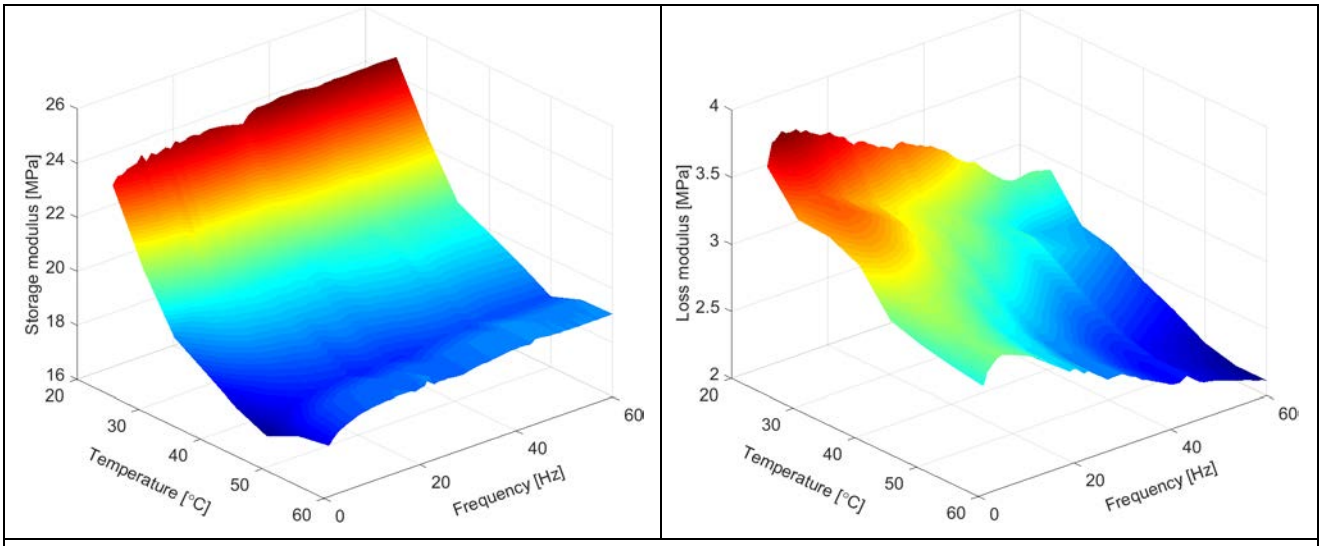

(a)

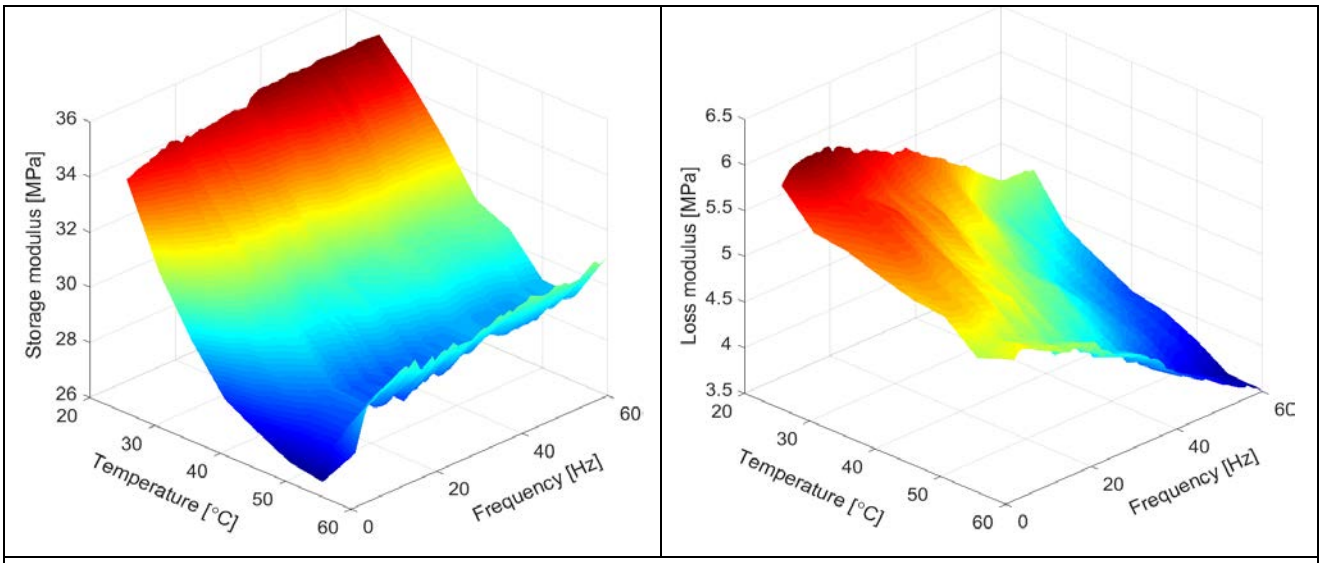

(b)

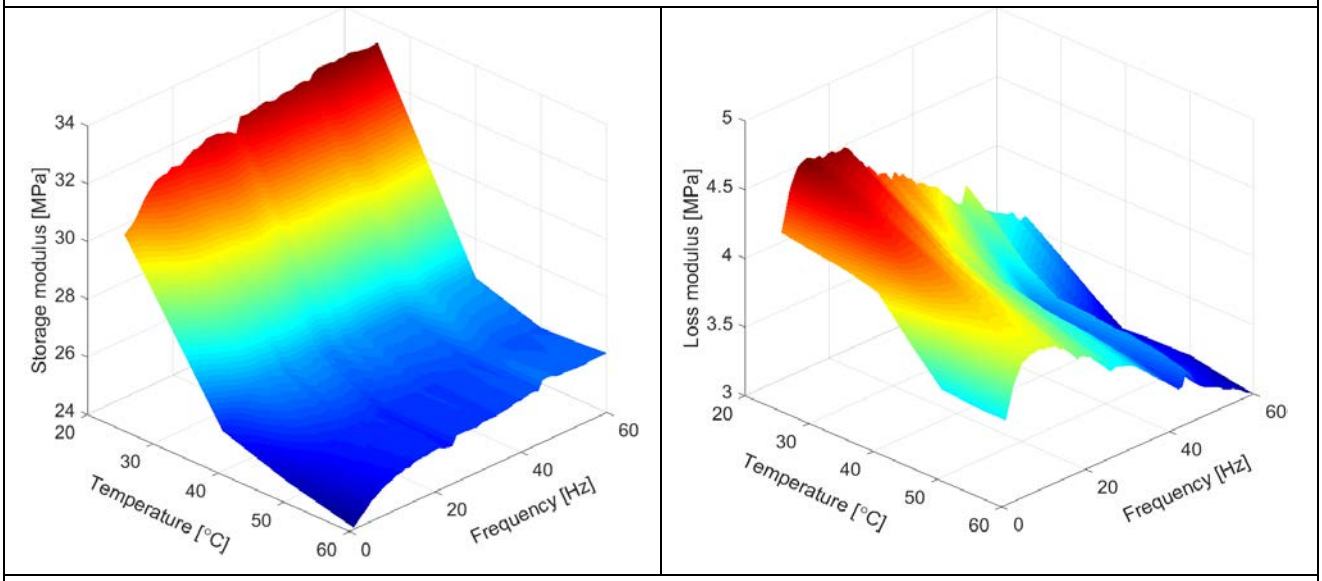

(c)

Figure 3. Frequency and temperature dependent dynamic modulus of the MRE sample under: (a) 0mT magnetic field (b) 0.25% strain amplitude and 300 mT magnetic field, and (c) 1% strain amplitude and 500 mT magnetic field.

Figure 3 shows the frequency and temperature dependent dynamic modulus and loss factor of the MRE samples under uniaxial harmonic compression with different strain amplitudes and magnetic fields. It was found that the variation of the dynamic modulus with temperature can be divided into two stages from room temperature (about 25°C) to 60°C. It initially decreased with temperature from room temperature to 50°C, and then started to increase or maintain a stable value until 60°C. The loss factor decreased with the increasing of temperature and the decrement of the curves was more remarkable when the MRE samples were under both magnetic field and higher temperature. The transition behavior happened at about 50°C is partly due to the phase transition of the silicon rubber matrix [10]. The MRE sample became soft at about 50°C and reached the exothermic peaks at 58.66°C according to the DSCthermal analysis result.

4.2 Applicablity of the time-temperature superposition principle

The time-temperature superposition (TTS) principle holds for the thermorheologically simple materials [27] and have been extended to a multi-component system in which some components have the same temperature dependence and the others have no temperature dependence [32, 33]. Therefore, the applicability of the TTS principle should be verified before the construction of the master curve. The Cole-Cole plot and the Black diagram (also called the van Gurp-Palmen plot) are two simple methods to verify whether the viscoelastic material is thermorheologically simple or not.

When the Cole-Cole plot and the Black diagram form a single smooth curve, the material is thermorheologically simple. The elastic constants are independent of temperature and the time constatnts have the same dependence of temperature. The isotherms of dynamic modulus can be shifted into a unique master curve by using the horizontal shift factor [28-30]. When the Cole-Cole plot and the Black diagram are temperature dependent, the material does not exhibit simple thermorheological behavior. Both horizontal and vertical shift factors should be applied to construct the master curve based on TTS principle [31, 32, 45].

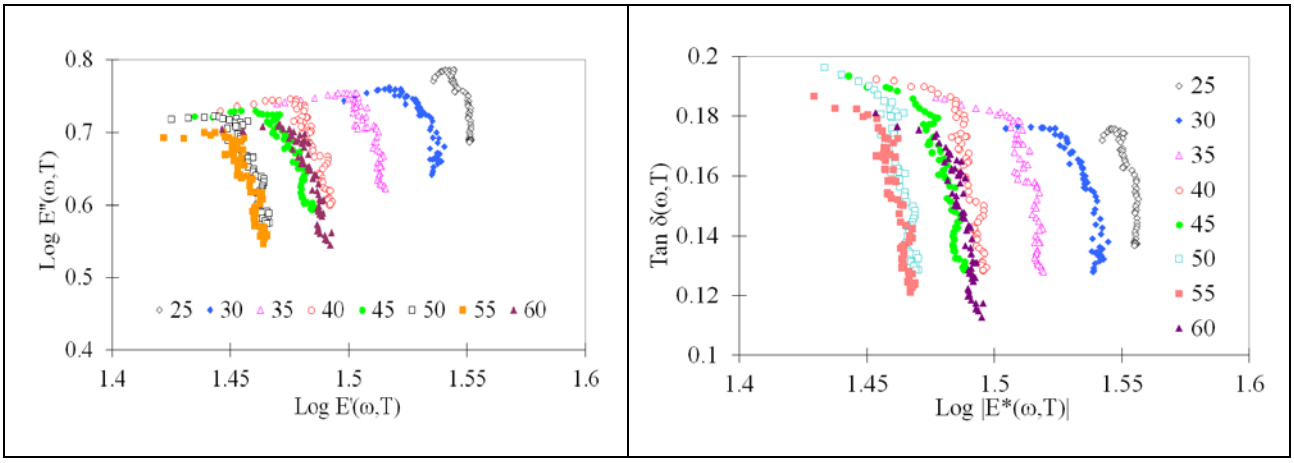

(a) (b)

Figure 4. (a) The Cole-Cole plot, and (b) the Black diagrams of the MRE samples under 0.25% uniaxial harmonic compression and 300 mT magnetic field.

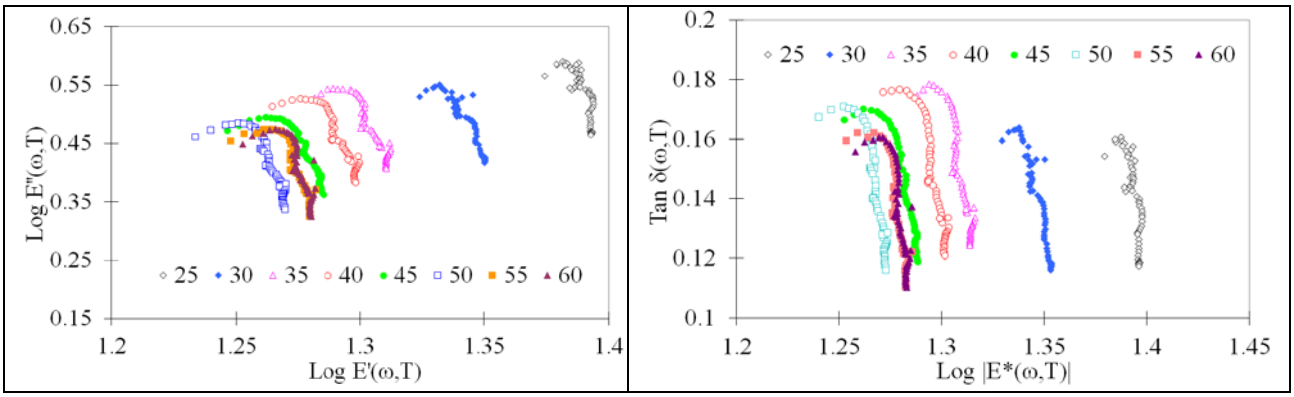

(a) (b)

Figure 5. (a) The Cole-Cole plot, and (b) the Black diagrams of the MRE samples under 1% uniaxial harmonic compression and non-magnetic field.

Figure 4 and Figure 5 show the logarithmic Cole-Cole plot and the semi-logarithmic Black diagram of the DMA measurement data of MRE samples under 0.25% uniaxial harmonic compression in the presence of 300 mT magnetic field and the samples subjected to 1% uniaxial harmonic compression in the absence of a magnetic field respectively. It can be observed that the logarithmic Cole-Cole plot and the semi-logarithmic Black diagram did not form a single smooth curve, but the sets of each curve were dependent on temperature and exhibited a similar shape at different temperatures. This indicated

that the MRE samples were not thermorheologically simple material, but the TTS may be applied to construct the master curve by using the horizontal shift factor and vertical shift factor [31, 32, 45].

In fact, the isothermal curves with a similar shape in Figure 4 and Figure 5 can be merged respectively into a single curve (as shown in Figure 6 and Figure 7) at a reference temperature of 40°C by applying the vertical shift factor. The similar shape of the Wicket plot obtained in Figure 6 and Figure 7 indictes that the TTS can be applied to construct the dynamic modulus master curve of the MRE samples under uniaxial harmonic compression within linear viscoelastic region. The scatter of calculated data in Figure 6 and Figure 7 are partly caused by the measurement noise. This graphical representation may assist in enhancing data analysis with measurement noise removal [29].

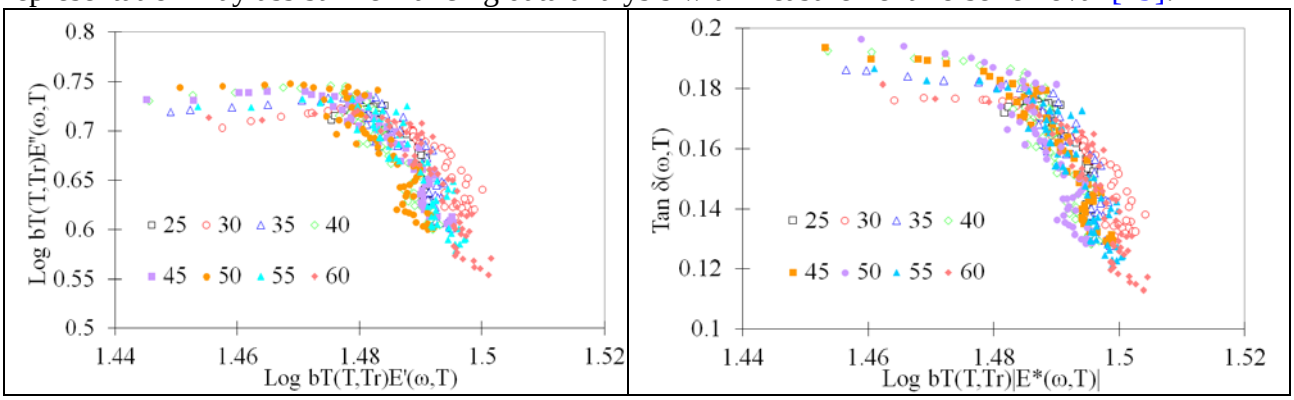

(a) (b)

Figure 6. The wicket plot calculated by applying the vertical shift factor to: (a) Cole-Cole plot, and (b) the Black diagrams of the MRE samples under 0.25% uniaxial harmonic compression and 300 mT magnetic field.

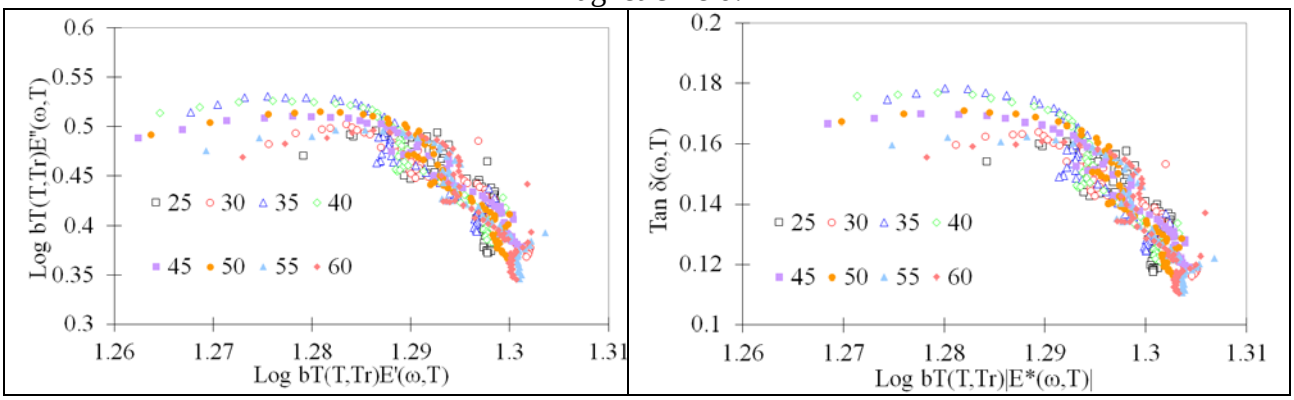

(a) (b)

Figure 7. The wicket plot calculated by applying the vertical shift factor to: (a) Cole-Cole plot, and (b) the Black diagrams of the MRE samples under 1% uniaxial harmonic compression and non-magnetic field.

4.3 Master curve construction

The dynamic modulus master curve of the MRE samples is constructed by applying the TTS principle at a reference temperature of 30°C. The model parameters for master curve and the numerical shift factors for each individual dynamic modulus are identified by minimizing the sum of square of error (SSE) between the predicted and measured data.

$$SSE = \sum \left(1 - \frac{E'_{pred}}{E'_{exp}}\right)^2 + \sum \left(1 - \frac{E''_{pred}}{E''_{exp}}\right)^2 \quad (12)$$

in which, (E'_{exp}, E'_{pred}) and (E''_{exp}, E''_{pred}) are experimental and predicted data of the storage modulus and loss modulus respectively.

The frequency dependent storage modulus and loss modulus at different temperatures as shown in

Figure 8 and Figure 10 are merged respectively into the master curves by using the horizontal and vertical shift factors. Figure 9 shows the dynamic modulus master curves of the MRE samples subjected to uniaxal harmonic compression with small strain amplitude of 0.25% in the magnetic field of 300 mT. Figure 11 shows the dynamic modulus master curves of the MRE samples subjected to 1% strain amplitude harmonic compression in absence of magnetic field. A reasonable good superposition of frequency and temperature is observed despite a few points are not superposition well with the others and deviate from the master curve. The goodness-of-fit parameters in Table 1 and Table 2, the standard error ratio (S_e/S_y) and the coefficient of determination (R^2), indicate that the excellent fitting results of loss modulus master curve and good fitting results of storage modulus master curve are obtained.

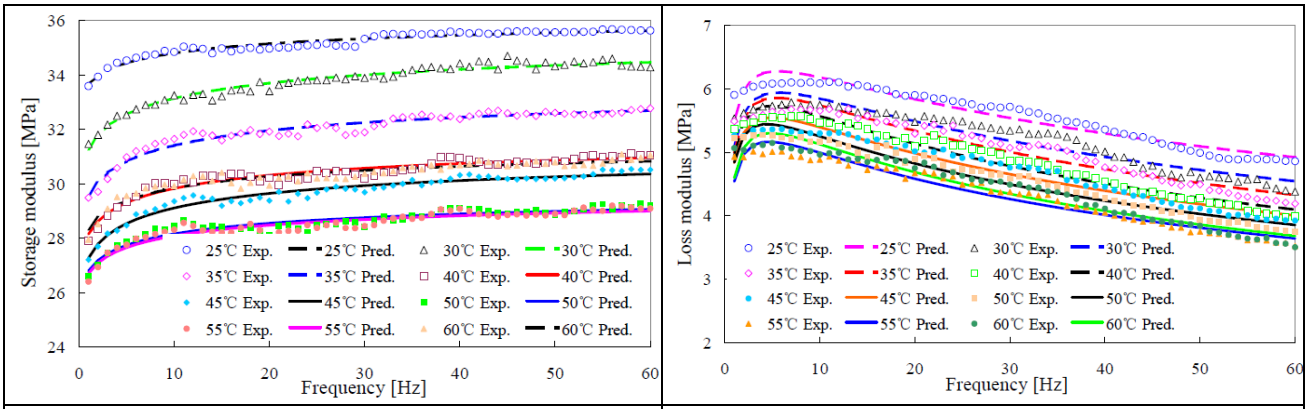

(a) (b)

Figure 8. Comparison between experimental and predicted data of: (a) storage modulus, and (b) loss modulus of the MRE samples under 0.25% strain amplitude and 300 mT magnetic field.

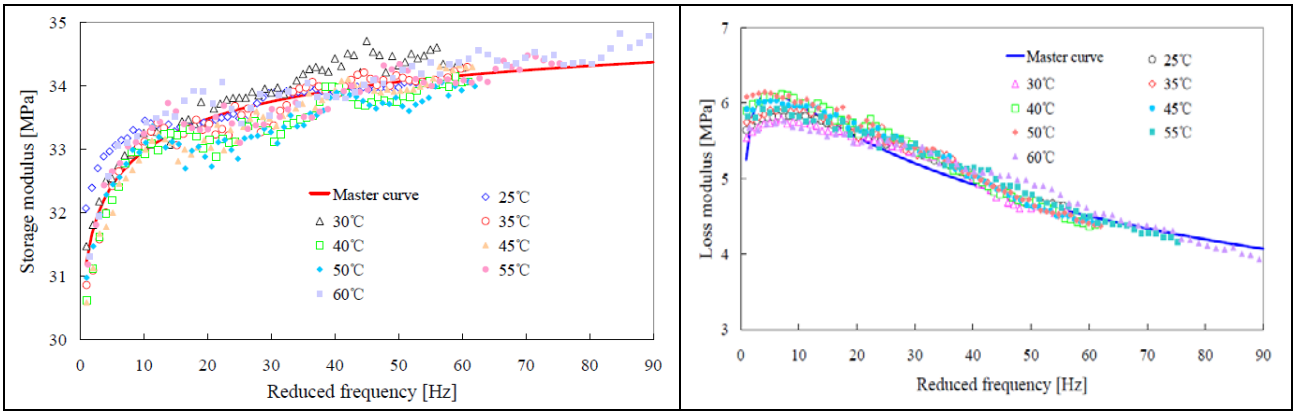

(a) (b)

Figure 9. Dynamic modulus master curve of the MRE samples under 0.25% strain amplitude and 300 mT magnetic field, (a) storage modulus, and (b) loss modulus.

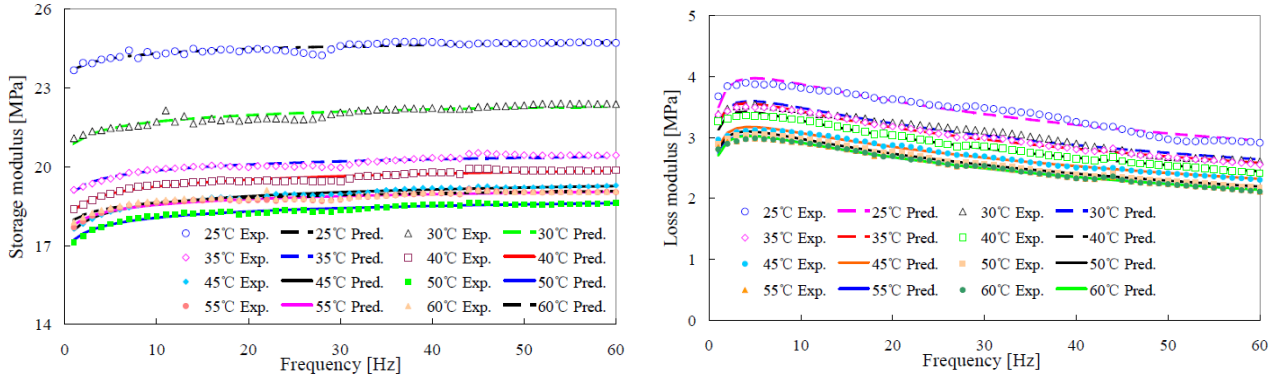

(a) (b)

Figure 10. Comparison between experimental and predicted data of: (a) storage modulus, and (b) loss modulus of the MRE samples under 1% strain amplitude and non-magnetic field.

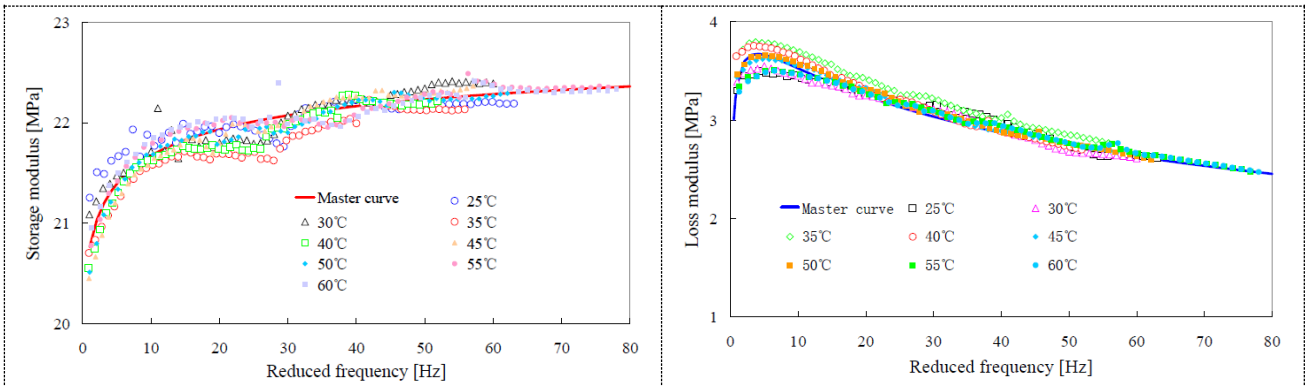

(a) (b)

Figure 11. The frequency and temperature dependent (a) storage modulus and (b) loss modulus of the MRE samples under 1% strain amplitude and non-magnetic field.

The goodness-of-fit statistical analysis results of the temperature dependent dynamic modulus and the fitting results by the fractional Zener model as shown in Figure 8 and Figure 10 are also presented in Table 1 and table 2 for comparative analysis. The master curve and the fractional Zener model fitting have similar correlations between experimental and predicted data of storage modulus and loss modulus. It indicates that the points deviate from the master curve is partly due to the fitting results of the fractional Zener model.

Table 1. Goodness-of-fit analysis of the master curve and the fractional Zener model for the MRE sample under uniaxial compression with 0.25% strain amplitude in the magnetic field of 300mT.

		25℃	30℃	35℃	40℃	45℃	50℃	55℃	60℃	Master curve
Storage modulus	S_eS_y	0.263	0.208	0.250	0.290	0.228	0.365	0.349	0.320	0.399
	R^2	0.937	0.960	0.942	0.923	0.952	0.878	0.888	0.906	0.847
Loss modulus	S_eS_y	0.273	0.317	0.281	0.227	0.249	0.230	0.239	0.271	0.293
	R^2	0.932	0.908	0.928	0.953	0.943	0.951	0.948	0.933	0.917

Table 2. Goodness-of-fit analysis of the master curve and the fractional Zener model for the MRE sample under uniaxial compression with 1% strain amplitude in absence of magnetic field.

		25℃	30℃	35℃	40℃	45℃	50℃	55℃	60℃	Master curve
Storage modulus	S_eS_y	0.398	0.386	0.307	0.239	0.136	0.189	0.252	0.303	0.359
	R^2	0.853	0.861	0.912	0.947	0.983	0.967	0.941	0.915	0.876
Loss modulus	S_eS_y	0.221	0.183	0.100	0.103	0.104	0.085	0.103	0.097	0.252
	R^2	0.954	0.969	0.991	0.990	0.990	0.993	0.990	0.991	0.939

4.4 Goodness-of-fit statistics of shift factors

The numerical shift factor presented the best fit between experimental and predicted data in the construction of the dynamic modulus master curve as shown in Table 1 and Table 2. However the functional shift factor, especially those with some thermodynamic basis, are still preferred to use because they are rapid and easy to apply in computer software [42, 43]. Figure 12 and Figure 13 show the comparison beween the numerical shift factors and the functional shift factors for constructing the dynamic modulus master curve of the MRE samples under uniaxial harmonic compression. The functional horizontal shift factor consist of the WLF empirtical equation, the Arrhenius equation, and the quadratic polynomial function. The DMA experiment results in Figure3 indicated that the viscoelastic behavior of the MRE samples under uniaxial compression can be identified into two regions by the transition temperaturere (about 50℃). The DMA measurement data within the temperature range of 25℃ to 50℃ are considered for the application of the Arrhenius equation and the WLF empirtical equation according to their thermodynamic basis.

Figure 12 and Figure 13 plot the numerical and functional shift factors versus temperature. It is clearly observed that the quadratic equation presents the excellent correlation between the numerical and the functional vertical shift. The statistical analysis results show that that standard error ratio S_e/S_y is less than 0.2 and the coefficient of determination R^2 is greater than 0.96. A little difference exists between the numerical and the functional horizontal shift factor. However, the Goodness-of-fit parameters of the resulting dynamic modulus master curve in Table 3 reveal that the functional horizontal shift factor works well for constructing the dynamic modulus master curve of the MRE samples under uniaxial harmonic compression. They present the excellent fitting results of the loss modulus master curve and the good fitting results of the storage modulus master curve respectively.

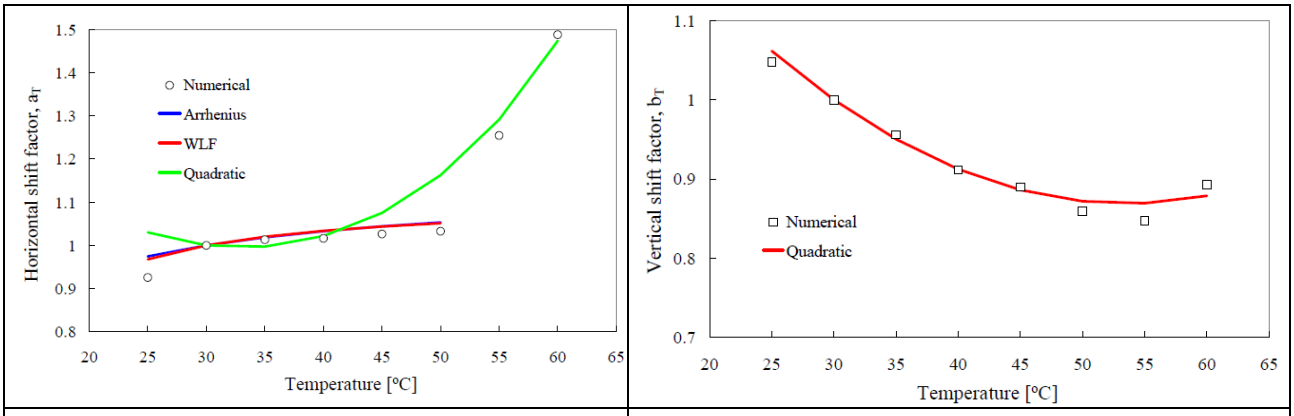

(a) (b)

Figure 12. Comparison between numerical and functional shift factors: (a) horizontal shift factor and vertical shift factor of the MRE samples under 0.25% strain amplitude and 300 mT magnetic field.

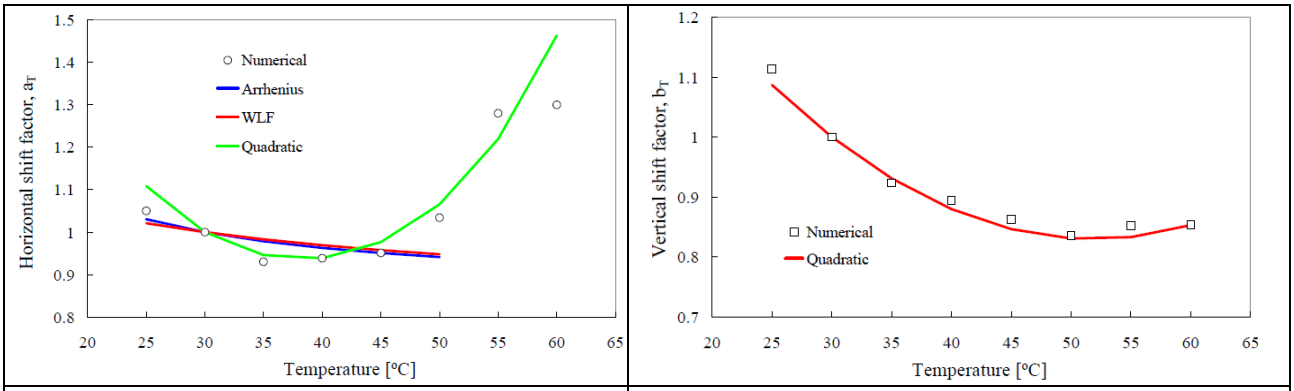

(a) (b)

Figure 13. Comparison between numerical and functional shift factors: (a) horizontal shift factor and vertical shift factor of the MRE samples under 1% strain amplitude and non-magnetic field.

Table 3. Goodness-of-fit parameters of the dynamic modulus master curve constructed by different horizontal shift factors

			numerical	WLF equation	Arrhenius equation	Quadratic polynomial
MRE under 0.25% and 300 mT	Storage modulus	S_eS_y	0.393	0.440	0.440	0.484
		R^2	0.852	0.809	0.809	0.769
	Loss modulus	S_eS_y	0.278	0.285	0.285	0.278
		R^2	0.926	0.920	0.920	0.924
MRE under 1% and 0 mT	Storage modulus	S_eS_y	0.328	0.469	0.464	0.408
		R^2	0.896	0.784	0.788	0.836
	Loss modulus	S_eS_y	0.198	0.245	0.243	0.221
		R^2	0.962	0.941	0.922	0.952

5 Conclusions

In this paper, the temperature dependent viscoelastic properties of the anisotropic MRE samples were measured by DMA experiments in different frequencies and magnetic fields. The applicability of the TTS principle was verified to the MRE samples under uniaxial harmonic compression and magnetic field by the logarithmic Cole-Cole plot and the semi-logarithmic Black diagram. To our knowledge, it is the first time that the dynamic modulus master curve of the MRE samples in the presence of magnetic field was constructed by the horizontal and vertical shift factors. The good correlations between the measured and predicted data were confirmed by performing statistical analysis for the goodness of fit. The constructed master curve and sgift factors can be used to predict the viscoelastic properties of the MREs beyond the DMA experiment range of temperatures and frequencies.

The obtained results show that there was a transition behavior of the MREs at about $50°C$ for dynamic modulus. The storage modulus of the MREs initially decreased with the increment of temperature up to $50°C$ and then increased with further increasing temperature. The transition temperature happens at about 50 °C may be regarded as a result of the superposition of two factors: the alpha phase transition of the particle reinforced silicone rubber and the dipole interaction between iron particles under the magnetic field when the silicon rubber matrix become soft due to the temperature elevation. The TTS principle can be applied to construct the dynamic modulus master curve of the MREs by using the horizontal shift factor and vertical shift factor when the Cole-Cole plot and the Black diagram exhibited a similar shape at different temperatures. The WLF empirical equation and the Arrhenius equation worked well for the horizontal shift factor before the transition temperature. While the quadratic polynomial function produced the excellent fitting results of the vertical shift factor and the good fitting results of the horizontal shift factor respectively within the DMA test temperature range. The excellent and good correlation between DMA experiment data and predicted results of the loss modulus and the storage modulus were evaluated respectively by the goodness-of-fit statistical analysis.

Acknowledgement

This work is supported by Lloyd's Register foundation.**Reference**

[1] Liao G J, Gong X L, Kang C J and Xuan S H 2011 The design of an active-adaptive tuned vibration absorber based on magnetorheological elastomer and its vibration attenuation performance *Smart Mater. Struct.* 20 075015

[2] Molchanov V S, Stepanov G V, Vasiliev V G, Kramarenko E Y, Khokhlov A R, Xu Z D and Guo Y Q 2014 Viscoelastic properties of magnetorheological elastomers for damping applications *Macromol. Mater. Eng.* 299 116-125

[3] Yang J, Sun S H, Tian T F, Li W H, Du H P, Alici G and Nakano M 2016 Development of a novel multi-layer MRE isolator for suppression of building vibrations under seismic events *Mech. Syst. Sign. Process* 70-71 811-820

[4] Bornassi S and Navazi H M 2018 Torsional vibration analysis of a rotating tapered sandwich beam with magnetorheological elastomer core *J. Intell. Mater. Syst. Struct.* 29 2406-2423

[5] Qiao X Y, Lu X S, Gong X L, Yang T, Sun K and Chen X D 2015 Effect of carbonyl iron concentration and processing conditions on the structure and properties of the thermoplastic magnetorheological elastomer composites based on poly(styrene-b-ethylene-co-butyleneb-styrene) (SEBS) *Polym. Test* 47 51-58

[6] Boczkowska A and Awietjan S F 2011 Effect of the elastomer stiffness and coupling agents on rheological properties of magnetorheological elastomers *WIT Trans. Eng. Sci.* 72 263-274

[7] Sapouna K, Xiong Y P and Shenoi R A 2017 Dynamic mechanical properties of isotropic/anisotropic silicon magnetorheological elastomer composites *Smart Mater. Struct.* 26 115010
[8] Schubert G and Harrison P 2015 Large-strain behaviour of magneto-rheological elastomers tested under uniaxial compression and tension, and pure shear deformations *Polym. Test* 42 122-134.
[9] Małecki P, Krolewicz M, Krzak J, Kaleta J, and Pigłowski J 2015 Dynamic mechanical analysis of magnetorheological composites containing silica-coated carbonyl iron powder *J. Intell. Mater. Syst. Struct.* 26 1899-1905
[10] Zhang W, Gong X L, Xuan S H and Jiang W Q 2011 Temperature-dependent mechanical properties and model of magnetorheological elastomers *Ind. Eng. Chem. Res.* 50 6704-6712
[11] Yu M, Zhao L J, Fu J and Zhu M 2016 Thermal effects on the laminated magnetorheological elastomer isolator *Smart Mater. Struct.* 25 115039
[12] Li W H, Zhou Y and Tian T F 2010 Viscoelastic properties of MR elastomers under harmonic loading *Rheol. Acta* 49 733-740
[13] Zhu J T, Xu Z D and Guo Y Q 2012 Magnetoviscoelasticity parametric model of an MR elastomer vibration mitigation device *Smart Mater. Struct.* 21 075034
[14] Guo F, Du C B and Li R P 2014 Viscoelastic parameter model of magnetorheological elastomers based on Abel dashpot *Adv. Mech. Eng.* 2014 629386
[15] Chen L and Jerrams S 2011 A rheological model of the dynamic behavior of magnetorheological elastomers *J. Appl. Phys.* 110 013513
[16] Blom P and Kari L 2011 A nonlinear constitutive audio frequency magneto-sensitive rubber model including amplitude, frequency and magnetic field dependence *J. Sound Vib.* 330 947-954
[17] Eem S H, Jung H J and Koo J H 2012 Modeling of magneto-rheological elastomers for harmonic shear deformation *IEEE Trans. Magn.* 48 3080-3083
[18] Behrooz M, Wang X J and Gordaninejad F 2014 Modeling of a new semi-active/passive magnetorheological elastomer isolator *Smart Mater. Struct.* 23 45013
[19] Kaleta J, Lewandowski D and Zietek G 2007 Inelastic properties of magnetorheological composites: II. Model, identification of parameters *Smart Mater. Struct.* 16 1954-1960
[20] Xin F L, Bai X X and Qian L J 2016 Modeling and experimental verification of frequency-, amplitude-, and magnetodependent viscoelasticity of magnetorheological elastomers *Smart Mater. Struct.* 25 105002
[21] Norouzi M, Alehashem S M S, Vatandoost H, Ni Y Q and Shahmardan M M 2016 A new approach for modeling of magnetorheological elastomers *J. Intell. Mater. Syst. Struct.* 27 1121-1135
[22] Wang Q, Dong X F, Li L Y and Ou J P 2018 Mechanical modeling for magnetorheological elastomer isolators based on constitutive equations and electromagnetic analysis *Smart Mater. Struct.* 27 065017
[23] Agirre-Olabide I, Kuzhir P and Elejabarrieta M J 2018 Linear magneto-viscoelastic model based on magnetic permeability components for anisotropic magnetorheological elastomers *J. Magn. Magn. Mater.* 446 155-161
[24] Nadzharyan T A, Kostrov S A, Stepanov G V and Kramarenko E Y 2018 Fractional rheological models of dynamic mechanical behavior of magnetoactive elastomers in magnetic fields *Polym.* 142 316-329
[25] Bai J B, Shenoi R A and Xiong J J 2017 Thermal analysis of thin-walled deployable composite boom in simulated space environment *Compos. Struct.* 173 210-218
[26] Alcock B, Cabrera N O, Barkoula N M, Reynolds C T, Govaert L E and Peijs T 2007 The effect of temperature and strain rate on the mechanical properties of highly oriented polypropylene tapes and all-polypropylene composites *Compos. Sci. Technol.* 67 2061-2070

[27] Tschorgl N W, Kbauss W G and Emrischoegl I 2002 The effect of temperature and pressure on the mechanical properties of thermo- and/or piezorheologically simple polymeric materials in thermodynamic equilibrium – A critical review *Mech Time-Depend Mater* 6 53-99
[28] Madigosky W M 2006 A method for modeling polymer viscoelastic data and the temperature shift function *J. Acoust. Soc. Am.* 119 3760-3765
[29] Moreira R A S, Corte-Real J D and Rodrigues J D 2010 A generalized frequency-temperature viscoelastic model *Shock Vib.* 17 407-418
[30] Rouleau L, Pirk R, Pluymers B and Desmet W 2015 Characterization and modeling of the viscoelastic behavior of a self-adhesive rubber using dynamic mechanical analysis tests *J. Aerosp. Technol. Manag.* 7 200-208
[31] Guedes R M 2011 A viscoelastic model for a biomedical ultra-high molecular weight polyethylene using the time–temperature superposition principle *Polym. Test* 30 294-302
[32] Nakano T 2013 Applicability condition of time–temperature superposition principle (TTSP) to a multi-phase system *Mech Time-Depend Mater* 17 439-447
[33] Çakmak U D, Hiptmair F and Major Z 2014 Applicability of elastomer time-dependent behavior in dynamic mechanical damping systems *Mech Time-Depend Mater* 18 139-151
[34] Agirre-Olabide I and Elejabarrieta M J 2016 Maximum attenuation variability of isotropic magnetosensitive elastomers *Polym. Test* 54 104-113
[35] Chooi W W and Oyadiji S O 2005 Characterizing the effect of temperature and magnetic field strengths on the complex shear modulus properties of magnetorheological (MR) fluid *Int. J. Modern Phys. B* 19 1318-1324.
[36] Böse H and Röder R 2009 Magnetorheological elastomers with high variability of their mechanical properties *J. Phys. Conf. Ser.* 149 012090
[37] Kaleta J, Królewicz M and Lewandowski D 2011 Magnetomechanical properties of anisotropic and isotropic magnetorheological composites with thermoplastic elastomer matrices *Smart Mater. Struct.* 20 085006
[38] Lokander M and Stenberg B 2003 Performance of isotropic magnetorheological rubber materials *Polym. Test* 22 245-251
[39] Davis L C 1999 Model of magnetorheological elastomers *J. Appl. Phys.* 85 3348-3351
[40] Kontou E and Katsourinis S 2016 Application of a fractional model for simulation of the viscoelastic functions of polymers *J. Appl. Polym. Sci.* 133 43505
[41] Dinzart F and Lipinski P 2009 Improved five-parameter fractional derivative model for elastomers *Arch Mech.* 61 459-474
[42] Yusoff N I M, Chailleux E and Airey G D 2011 A comparative study of the influence of shift factor equations on master curve construction *Int. J. Pav. Res. Technol.* 4 324-336
[43] Rowe G M and Sharrock M J 2011 Alternate shift factor relationship for describing temperature dependency of viscoelastic behavior of asphalt materials *Transp. Res. Rec.* 2207 125-135
[44] Kim M, Mohammad L N and Elseifi M A 2015 Effects of various extrapolation techniques for abbreviated dynamic modulus test data on the MEPDG rutting predictions *J. Mar. Sci. Technol.* 23 353-363
[45] Dealy J and Plazek D 2009 Time-temperature superposition – a user'susers guide *Rheol. Bull.* 78 16-31